







Article

Treated Unconventional Waters Combined with Different Irrigation Strategies Affect ¹H NMR Metabolic Profile of a Monovarietal Extra Virgin Olive Oil

Federica Angilè ^{1,2}, Gaetano Alessandro Vivaldi ^{3,*} , Chiara Roberta Girelli ¹ , Laura Del Coco ¹ , Gabriele Caponio ³ , Giuseppe Lopriore ⁴, Francesco Paolo Fanizzi ^{1,5,*}  and Salvatore Camposeo ³ 

- ¹ Dipartimento di Scienze e Tecnologie Biologiche e Ambientali, Università del Salento, Via Monteroni, 73100 Lecce, Italy; federica.angile@unisalento.it (F.A.); chiara.girelli@unisalento.it (C.R.G.); laura.delcoco@unisalento.it (L.D.C.)
- ² Centro di Ricerca Olivicoltura, Frutticoltura e Agrumicoltura, Contrada Li Rocchi Vermicelli 83, 87036 Rende, Italy
- ³ Dipartimento di Scienze Agro-Ambientali e Territoriali, Università degli Studi di Bari Aldo Moro, Via Amendola 165/a, 70126 Bari, Italy; gabriele.caponio@uniba.it (G.C.); salvatore.camposeo@uniba.it (S.C.)
- ⁴ Dipartimento di Scienze Agrarie, degli Alimenti e dell'Ambiente, Università di Foggia, Via Napoli 25, 71121 Foggia, Italy; giuseppe.lopriore@unifg.it
- ⁵ Consorzio Interuniversitario di Ricerca in Chimica dei Metalli nei Sistemi Biologici, Piazza Umberto I 1, 70121 Bari, Italy
- * Correspondence: gaetano.vivaldi@uniba.it (G.A.V.); fp.fanizzi@unisalento.it (F.P.F.); Tel.: +39-080-5442982 (G.A.V.); +39-0832-299265 (F.P.F.)



Citation: Angilè, F.; Vivaldi, G.A.; Girelli, C.R.; Del Coco, L.; Caponio, G.; Lopriore, G.; Fanizzi, F.P.; Camposeo, S. Treated Unconventional Waters Combined with Different Irrigation Strategies Affect ¹H NMR Metabolic Profile of a Monovarietal Extra Virgin Olive Oil. *Sustainability* **2022**, *14*, 1592. <https://doi.org/10.3390/su14031592>

Academic Editor: Jan Hopmans

Received: 31 December 2021

Accepted: 27 January 2022

Published: 29 January 2022

Publisher's Note: MDPI stays neutral with regard to jurisdictional claims in published maps and institutional affiliations.



Copyright: © 2022 by the authors. Licensee MDPI, Basel, Switzerland. This article is an open access article distributed under the terms and conditions of the Creative Commons Attribution (CC BY) license (<https://creativecommons.org/licenses/by/4.0/>).

Abstract: The agricultural sector is facing a decrease in water supply and water quality at a global level and this is a problem that strictly affects all the Mediterranean olive growing areas. The aim of this work was to evaluate, for the first time, by NMR Spectroscopy and multivariate data analysis the metabolic profiling of the oils produced under different irrigation schemes. Arbosana olive oils were obtained from the use of saline reclaimed water (RW) and treated municipal wastewater (DW), combined with: full irrigation (FI) and regulated deficit irrigation (RDI). The results show a higher relative content of saturated fatty acids in EVOOs obtained from RDI strategy, regardless of the water source. Moreover, an increase in unsaturated fatty acids, a $\omega 6/\omega 3$ ratio content was observed in EVOOs obtained from RW when compared with DW water. Furthermore, the RW–RDI showed an increase in secoiridoid derivatives and hydroperoxides with respect to DW–RDI. A sustainable irrigation management, by combining a deficit irrigation strategy and saline reclaimed water source, could be crucial in order to overcome the problem of water scarcity and to guarantee the olive oil nutraceutical properties. The ¹H NMR-based metabolomic approach proved a powerful and versatile tool for this specific investigation.

Keywords: extra virgin olive oil; DESERT technology; regulated deficit irrigation; fatty acids; phenolic compounds; oxidation compounds; NMR; chemometrics approach

1. Introduction

To date, climate change is considered one of the major concerns for society, as reported by the Global Risk Report 2020 [1]. In particular, the duration, maximal temperature and global intensity of heat waves together with droughts have strongly increased over the past 30 years [2], thus representing the greatest risk. The economic loss, due to water scarcity, involves several productive areas of the agriculture sector. In particular, in the Italian context, a EUR 2 billion loss was estimated for agricultural farms [2]. Availability of water for irrigation is a key factor for the agricultural sector of the Apulia region (Southern Italy), this land being characterized by a Mediterranean climate with hot, dry summers and mild, wet winters [2,3]. In the Apulia region, a high irrigation water volume is required to supply

many hectares of permanent crops (represented by olives, grapes and almonds) and fresh-cut vegetables. Overall, these crops account for 80% of the region's agricultural irrigated land [3]. In addition to drought, local farmers further reduced the availability of water for agriculture by the effects of drilling more than 200,000 wells [4]. This resulted in a gradual salinization and depletion of considerable water storage originally intended for agricultural purposes [2,5]. Thus, several strategies in order to safeguard the water availability are needed [6]. The deficit irrigation techniques (DI), combined with the use of unconventional water sources are potential strategies in order to make sustainable this natural no-renewable resource use [5–7]. DI represents a useful technique to reduce the problem of water scarcity for agriculture by reducing irrigation volumes during phenological phases, when the plant is the least sensitive to water stress, with little impact on fruit yield or quality [5]. During DI application, the irrigation regime is monitored in order to optimize water productivity. At the same time, positive economic returns to growers are guaranteed [7]. Moreover, reclaimed water represents an efficient alternative for irrigation in agriculture, since it is considered a non-expensive and reliable source [6,7]. Furthermore, reclaimed water represents a potential enhanced resource because it contains macronutrients that could be beneficial for crops [7] and might also reduce fertilizer application rates and increase growers income [8]. On the other hand, saline reclaimed water may cause risks to agriculture due to high salts content and toxic ionic and micropollutants levels that can accumulate in the soil and crops over time [5,9]. For these reasons, reducing salt concentration in reclaimed water at the levels of desalinated water could be an interesting option [7].

It is widely known that olive trees, being the main fruit tree crop in Italy, are characterized by high drought and salinity tolerance [7,10]. The olive tree salt tolerance is due to the ability of excluding potentially toxic ions at the root level and therefore regulating both ions concentration in xylem and toxic ions accumulation in aerial parts [11]. Several studies [7,11–14] demonstrated that tolerance to salinity strictly depends on olive varieties when trees are treated with reclaimed water. Moreover, olives and olive oils are the principal sources of fat in the Mediterranean diet and they appear to be an excellent example of functional foods [15,16]. In general, the olive oil quality depends on cultivar, pedoclimatic condition, agronomic techniques, storage conditions and mill extraction processing. DI modifies olive oil fatty acids content (in particular leading to a decrease in linoleic acid) [17], vegetative growth [18] and fruit quality [19]. At the same time, moderate water stress positively influences fruit maturity, oil yield and quality. The variability in lipid and phenolic profiles in olive oil is also related to cultivar, agronomic (irrigation, relative humidity and rainfall) and technological (oil extraction and storage) conditions [20]. Water source and irrigation strategies affect the polyphenols content of olive oils [21,22]. In general, agronomic and technological conditions, during extra virgin olive oil (EVOO) production, influence the content of secoiridoid derivatives. Operative conditions during crushing and separation are the principal aspects of the technological production process responsible for the secoiridoid content variations in EVOO [20]. Moreover, both fatty acids and phenolic compounds contents also depend on climate and the fruit ripening stage [23,24]. In particular, during ripening, the olive oil becomes less stable due to the decrease in phenolic compounds and increase in polyunsaturated fatty acids [23]. Early harvested fruit produces a more stable oil for antioxidant effects of phenolic compounds. On the other hand, excessive phenolic compound levels may result in unacceptable organoleptic characteristics of the product. The changes in lipid and phenolic content are reflected in the quality, oxidative stability, sensory characteristics and nutritional value of the olive oil. Thus, also setting criteria for the harvest date is very important for production efficiency and product quality [23,25], and in order to preserve the high nutraceutical value of olive oil [20,26–28]. Previous results show the effects of different irrigation strategies (FI: full irrigation; RDI: regulated deficit irrigation) combined with two qualities of reclaimed water (DW: desalinated water; RW: reclaimed water) on fruit yield and oil quality (fatty acid profiles and phenolic compounds content) of monovarietal Arbosana EVOOs [5]. On the

other hand, the use of an NMR based metabolomics approach in the study of hydric regime effects on agriculture products is unprecedented in the EVOOs field and limited to an application on zucchini cultivation [29]. Moreover, few works studied the effects of combination between the unconventional waters (DW and RW) use and two different irrigation approaches on the metabolic profile of olive oil, in particular on Arbosana EVOOs [5].

The aim of this work was to evaluate the metabolic profiling by Nuclear Magnetic Resonance (NMR) Spectroscopy and multivariate data analysis (MVDA) of the oils produced under the different irrigation schemes (RW–RDI, DW–RDI, RW–FI and DW–FI). ^1H NMR Spectroscopy is amply used in food analysis and it is a versatile approach used in metabolomics studies to evaluate food quality, such as olive oil [30]. In detail, the NMR-based metabolomics approach allows to observe both major (fatty acids) and minor components (phenolic compounds and derivatives) in EVOOs. The combination of NMR and the chemometrics approach can help to identify changes in metabolic profiles related to the contents of fatty acids and phenolic compounds content and oil stability. As far as we know, this is the first study where irrigation strategy and water source effects on olive oil characteristics have been investigated by Nuclear Magnetic Resonance (^1H NMR) metabolic profiling combined with multivariate data analysis (MVDA). According to the obtained data, this metabolomics approach has allowed to observe how the water quality and irrigation technique influence the olive oil quality. Thus, the right combination between irrigation strategy and specific water source is important in order to make sustainable this natural non-renewable resource use and to guarantee the olive oil shelf life and the nutraceutical properties of EVOOs as well.

2. Materials and Methods

2.1. Experimental Site and Irrigation Treatments

The research was performed in the DEsalination and SEnsoR Technology (DESERT) experimental field of the University of Bari (Apulia, $41^{\circ}06'41''$ N, $16^{\circ}52'57''$ E, 5 m above sea level), during the 2018 harvesting year. The crop used was 2-year self-rooted Arbosana olive trees planted in uncovered 100-L polyethylene pots (diameter, 50 cm; height, 65 cm) as already reported in Trigueros et al. 2019 [7].

According to Trigueros et al. 2019 [5], two irrigation water sources were examined. The first was a low-cost water DEsalination and SEnsoR Technology (DESERT) DW, a treated municipal wastewater obtained by treating secondary wastewater coming from Bari secondary wastewater treatment plant with electrical conductivity (EC_w) 1.2 dS m^{-1} by ultrafiltration, active carbon and reverse osmosis until reaching an EC_w of 1.0 dS m^{-1} [5]. The second was saline RW, obtained by mixing the secondary wastewater (EC_w 1.2 dS m^{-1}) with the brine produced in the DESERT prototype until reaching an EC_w of 3 dS m^{-1} . Moreover, two irrigation treatments were established for each water source. The first treatment was a full irrigation (FI) treatment throughout the growing season to fully satisfy crop water requirements (100% ET_c). The second one was a regulated deficit irrigation (RDI) treatment with an irrigation regime similar to FI, except during the first stage of oil accumulation, when half the water applied to the FI (50% ET_c) was used. The RDI period was chosen because it corresponded to approximately the end of maximum rate of pit hardening and before the rapid phase of fruit growth and oil accumulation begins, thus avoiding the fruit-set period (Stage 1) when olive trees are more sensitive to water stress [18,19]. The irrigation was scheduled on the basis of daily evapotranspiration of the crop (ET_c) accumulated during the previous week. ET_c values were estimated as recommended by FAO [5]. The RDI period started on DOY 180 (29 June 2018) and ended on DOY 243 (31 August 2018) and the seasonal irrigation volume applied was 2460 and $2011 \text{ m}^3 \cdot \text{ha}^{-1}$ for FI and RDI treatments, respectively, so that the RDI treatment saved about 21% of irrigation water [5].

2.2. Sampling and Oil Extraction

All the olives from each tree of each treatment (about 2 kg per tree) were harvested at the same ripening stage: pigmentation index of 1 and detachment index of 2 N g⁻¹, following the criteria already reported [5,23]. The oil was mechanically extracted and separated by vertical centrifugation (no solvent applied). All the oils fell into the chemical extra virgin category, with a free acidity of 0.25% as mean [5]. The 16 oil samples obtained (four samples for each treatment) were filtered and stored at 14 °C in a dark and cool place in amber glass until analysis; for each irrigation strategy, a number of eight oil samples (four each for DW-FI and RW-FI as well as four for DW-RDI and RW-RDI) were obtained and reported in Table 1. Three technical replicates were formed and analyzed for each oil sample for a total of 48 complete recorded ¹H NMR profiles.

Table 1. Summary of Arbosana olive oil samples. FI: full irrigation; RDI: regulated deficit irrigation; DW: desalinated water; RW: reclaimed water.

		Irrigation Strategy	
		FI	RDI
No-conventional water	DW	DW-FI 1	DW-RDI 5
		DW-FI 2	DW-RDI 6
		DW-FI 3	DW-RDI 7
		DW-FI 4	DW-RDI 8
	RW	RW-FI 9	RW-RDI 13
		RW-FI 10	RW-RDI 14
		RW-FI 11	RW-RDI 15
		RW-FI 12	RW-RDI 16

2.3. ¹H NMR Spectroscopy

For NMR analysis, ~140 mg of olive oil was dissolved in deuterated chloroform (CDCl₃) containing tetramethylsilane, TMS, 0.03% *v/v* as internal standard (0.00 ppm) in the proportion of olive oil-CDCl₃ (13.5:86.5, *w/w*). From the obtained mixture, a volume of 600 µL was transferred into a 5 mm NMR tube. NMR spectra were acquired on a Bruker Avance III spectrometer (Bruker, Karlsruhe, Germany) operating at 400.13 MHz for ¹H observation and 300.0 K, equipped with a BBI 5 mm inverse detection probe incorporating a z axis gradient coil. NMR experiments were performed under full automation for the entire process after loading each sample on a Bruker Automatic Samples Changer (BACS) interfaced with the software IconNMR (Bruker). Automated tuning and matching, locking and shimming, and calibration of the 90° hard pulse P(90°) were performed for individual samples using standard Bruker routines ATMA, LOCK, TOPSHIM and PULSECAL to optimize NMR conditions. For each sample, after a 5 min waiting period for temperature equilibration, two ¹H NMR experiments were performed: a standard one-dimensional (¹H ZG) NMR experiment and a one-dimensional 1D NOESYGPPS NMR pulse sequence (with suppression of the strong lipid signals for minor components enhancement). Measurements were repeated once in random order after completion of the first entire set. Spectra were obtained with the following conditions: zg Bruker pulse program (for ¹H ZG), 64K time domain (TD), spectral width (SW) of 20.5524 ppm (8223.685 Hz), a receiver gain (RG) of 4 and number scans (NS) of 16; noesygpps1d.comp2 Bruker pulse program (for 1D NOESYGPPS NMR), 32K TD, SW 20.5524 ppm, RG 16 and NS 32. ¹H spectra were obtained by the Fourier Transformation (FT) of the free induction decay (FID), applying an exponential multiplication with a line broadening factor of 0.3 Hz, automatically phased and baseline corrected. Chemical shifts were reported with respect to TMS signals set a 0.0 ppm, obtaining peak alignment. The metabolites were assigned on the basis of 1D NMR spectra analysis (¹H ZG, 1D NOESYGPPS) and by comparison with published data [31–33]. Fatty acid percentage

was calculated according to the procedure already reported in Barison, 2010 [34]. For minor components, signals corresponding to oleocanthal/oleacein (9.22 ppm), tyrosol and derivatives (6.78 ppm), hydroxytyrosol and derivatives (6.74 ppm), hydroperoxydes (8.18 ppm), hydroperoxy-(Z,E)-conjugated dienic system (6.58 ppm) and hydroperoxy-(E,E)-conjugated dienic system (5.74 ppm) were manually selected and integrated, using TMS, as well as the glycerol signals (4.33–4.26 ppm) as internal standard. The significant differences of the mean values, for all the treatments, were obtained by analysis of variance (one-way ANOVA), with Tukey's honestly significant differences (HSD) post hoc test, using the R software package, version 4.0.4, on a 64 bit Windows machine (R, Development Core Team, 2013) [35]. The levels of statistical significance were at p -values < 0.05 with a 95% confidence level. Furthermore, in order to calculate the absolute concentration of secoiridoid derivatives, the ERETIC 2 (electronic reference to access in vivo concentrations) methodology was used. For calibration, the reference sample (0.195 mol/L of 1,4 dioxane solution in CDCl_3) was used and the specific proton resonance at 3.70 ppm (s, 8H) was calibrated for analysis. Peak integration, Eretic measurements and spectrum calibration were obtained by the specific subroutines of Bruker Top-Spin 3.6.1 software [36].

2.4. Data Processing and Multivariate Statistical Analysis (MVDA)

The NMR spectra were processed using Topspin 3.6.1 and Amix 3.3.14 (Bruker, Biospin, Italy), checked by visual inspection and subjected to the successive bucketing process for multivariate statistical analyses. A rectangular bucketing of 0.04 width was performed within the spectral ranges 10.00–0.5 ppm region for ^1H ZG (BUCKET-1, 48 samples in rows and 221 variables in columns) and 10.00–5.50 ppm region for 1D NOESYGPPS (BUCKET-2, 48 samples in rows and 96 variables in columns), excluding the residual chloroform signals (7.6–6.9 ppm). In both cases, the total sum normalization was applied to minimize small differences due to sample concentration and/or experimental condition among samples. Moreover, each bucket in a bucket row reduced spectrum was labelled with the central chemical shift value for its specific 0.04 ppm width. The input variables used as descriptors for each sample in chemometric analyses are the buckets. The description of statistical analyses refers to Pareto-scaled data obtained by dividing the mean-centered bucket values by the square root of the standard deviation [37,38]. The two bucket tables (BUCKET-1 and BUCKET-2), obtained by alignment (using TMS for calibration at δ 0.00 ppm) and successive bucket row reduction in the spectra, were separately submitted to MVDA. MVDA was performed by using Simca-14 software (Sartorius Stedim Biotech, Umeå, Sweden). In particular, PCA (Principal Component Analysis) and OPLS-DA (Orthogonal Partial Least Squares Discriminant Analyses, respectively) analyses were applied to the data [37,38]. PCA is at the basis of the multivariate analysis [37,39] and usually performed to extract and display the systematic variation in a data matrix X formed by rows (the considered observations) and columns (the variables) of the buckets from each NMR spectrum. A PCA model provides a summary, or an overview, of all observations in the data table. The OPLS-DA analysis is a modification of the usual PLS-DA (partial least-squares discriminant analysis) method which filters out variation that is not directly related to the response and produces models of clearer interpretation, focusing the predictive information on one component. The further improvements made by the OPLS-DA in MVDA resides in the ability to separate the portion of the variance useful for predictive purposes from the not predictive variance (which is made orthogonal) [37]. Statistical models were validated using the internal cross-validation default method (seven-fold) and further evaluated with a permutation test, all available in the SIMCA-14 software [37,38]. The quality of the models was described by R^2 and Q^2 parameters [37]. The first (R^2) is a cross-validation parameter defined as the portion of data variance explained by the models and indicates the goodness of fit. R^2X and R^2Y represent the variance fraction of the X and Y matrix, respectively. The second (Q^2) represents the portion of variance in the data predictable by the model. The models with 3–5 components presented satisfactory total variance R^2 and predictive capability Q^2 values. The minimal number of components required can be easily

defined since R^2 and Q^2 parameters display a completely diverging behavior as the model complexity increases [37]. For these parameters, a value higher than about 0.5 indicates a good model. The results were shown by the optimal bi-dimensional scores plots and the corresponding loadings plots, these last were used to identify the molecular components responsible for separation among groups [30].

3. Results

3.1. MVDA Analysis (PCA and OPLS-DA) on EVOOs Major Components (BUCKET-1)

A preliminary unsupervised PCA was performed on the NMR data set, specifically related to the oil major components (BUCKET-1, obtained using ^1H ZG spectra), with the aim to observe the natural grouping of the data (Figure 1a). The PCA model revealed a degree of separation between the two irrigation strategies (RDI and FI). In order to confirm the separation between the two groups (RDI and FI) and identify the discriminating metabolites, a supervised multivariate analysis OPLS-DA was then performed (validated by the permutation test, Figure S1 in Supplementary Materials). In the OPLS-DA score plot, the predictive $t[1]$ component clearly separated the two groups (Figure 1b). From both the S-plot and S-line plot analysis of the OPLS-DA model (Figure 1c,d), it was possible to define the variables (chemical shifts of the bucket reduced NMR spectra) responsible for the observed separation. The NMR resonances accountable for the RDI and FI sample separation due to oil major components are also highlighted in the ^1H NMR spectrum (Figure S2 in Supplementary Materials). In particular, there was a high relative content of saturated fatty acids, while a relatively lower content of unsaturated oleic, linoleic and linolenic acids characterized RDI oil samples when compared with FI samples. Interestingly, in the OPLS-DA score plot, a certain degree of separation was also observed along the orthogonal component to $t[1]$, within each irrigation treatment group (intra-class separation). Specifically, both RDI and FI-originated samples resulted in two clearly separated subclusters on the basis of used water sources (RW and DW) (Figure 1b). A marked separation was shown by the two RDI subgroups, identified according to the used water source (DW-RDI and RW-RDI), while the two FI subgroups (DW-FI and RW-FI) still appeared as a homogeneous cluster.

Pairwise OPLS-DA Analysis According to Irrigation Strategy (RDI, FI) and Water Source (RW, DW) for EVOOs Major Components (BUCKET-1)

In order to evaluate the effects of both irrigation strategies (RDI, FI) and water sources used (RW, DW), a supervised pairwise analysis OPLS-DA for all the possible treatment combinations was performed, thus obtaining six different statistical models. In particular, two models were obtained for the used water sources (RW, DW) and each defined irrigation strategy ((RW vs. DW) (RDI conditions) and (RW vs. DW) (FI conditions)). Two models compared the different irrigation strategy for each defined water source used ((RDI vs. FI) (RW used source) and (RDI vs. FI) (DW used source)). Finally, two more models offered a cross-exchange comparison of the irrigation strategy and the water source strategy used (RW (FI conditions) vs. DW (RDI conditions) and RW (RDI conditions) vs. DW (FI conditions)).

The (RW vs. DW) (RDI conditions) OPLS-DA analysis, with one predictive and three orthogonal components (1 + 3 + 0), gave a good model, with a total variance of $R^2X = 0.787$, $R^2Y = 0.954$ and predictability to $Q^2 = 0.807$. In the OPLS-DA score plot, the olive oils obtained from DW and RW water source use were well separated along the predictive component $t[1]$ (Figure S3a in Supplementary Materials). The molecular components responsible for separation between olive oil samples were studied by examining the OPLS-DA S-plot (Figure S3a in Supplementary Materials).

The OPLS-DA analysis performed on (RW vs. DW) (FI conditions) samples gave a good model (1 + 3 + 0) with $R^2X = 0.771$, $R^2Y = 0.938$ and $Q^2 = 0.866$ (Figure S3b in Supplementary Materials), revealing a separation according to the non-conventional waters used, RW and DW. The buckets identifying the NMR signals responsible for the class separation are indicated in the S-plot of the OPLS-DA model (Figure S3b in Supplementary

Materials). In particular, for RDI treatment as well as FI, the olive oils obtained using DW water source were characterized by a high relative content of saturated fatty acids (1.26 ppm). However, considerably higher levels of unsaturated fatty acids, such as linoleic (2.74 and 5.34 ppm) and linolenic (2.78 and 5.38 ppm) acids, were observed in olive oil samples obtained using RW.

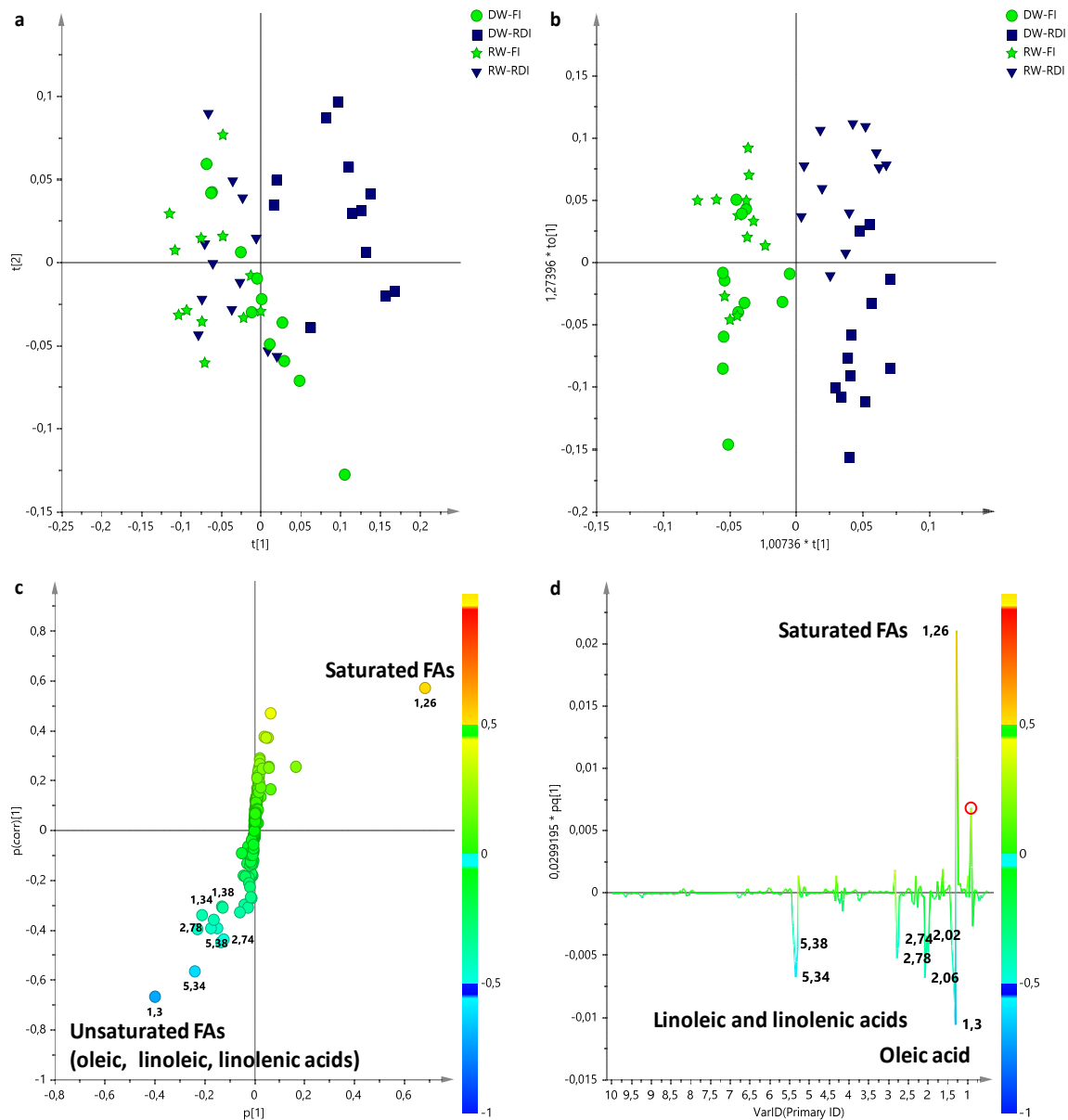


Figure 1. (a) $t[1]/t[2]$ PCA score plot (4 principal components, PCs, with more than 85% of the explained variance and $R^2X = 0.821$ and $Q^2 = 0.611$) performed on major components (BUCKET-1) of olive oil samples obtained from two irrigation strategies, FI and RDI. (b) OPLS-DA (1 + 3 + 0, $R^2X = 0.777$, $R^2Y = 0.866$, $Q^2 = 0.81$) $t[1]/to[1]$ score plot performed on major components (BUCKET-1) of olive oil samples obtained from two irrigation strategies, FI and RDI. (c) S-plot for the OPLS-DA model. (d) S-line for the OPLS-DA model. Green circle, DW-FI; blue box, DW-RDI; green star, RW-FI; blue triangle, RW-RDI. The variables indicated the chemical shift value (ppm) in the 1H NMR spectrum.

Focusing on the effect of the different irrigation strategies for a single used water source an OPLS-DA analysis was performed obtaining a new model (RDI vs. FI) (RW water source). The OPLS-DA, with one predictive and three orthogonal components (1 + 3 + 0), gave a

satisfactory model, having a total variance of $R^2X = 0.685$, $R^2Y = 0.939$ and predictability to $Q^2 = 0.817$. In the OPLS-DA score plot, the olive oils obtained from FI and RDI strategies were clearly separated along the predictive component $t[1]$ (Figure S3c in Supplementary Materials). The OPLS-DA performed on (RDI vs. FI) (DW conditions) gave a good model (1 + 3 + 0) with $R^2X = 0.824$, $R^2Y = 0.958$ and $Q^2 = 0.892$. In the OPLS-DA score plot, the olive oil samples resulted in clear separations along the predictive component $t[1]$, according to irrigation strategy RDI and FI (Figure S3d in Supplementary Materials). The S-plots for the models revealed the difference discriminating between the major component profiles of the considered classes of olive oils (Figure S3c,d in Supplementary Materials). Specifically, olive oils obtained with RDI irrigation strategy, in both RW and DW water sources, were characterized by a higher relative content of saturated fatty acids (1.26 ppm), while a higher relative content of unsaturated fatty acids (1.98 ppm) was found in olive oil obtained using the FI system. In particular, oleic acid (1.30 and 2.02 ppm), linoleic acid (2.74 and 5.34 ppm) and linolenic acid (2.78 and 5.38 ppm) were found as the most discriminating compounds.

Finally, the models obtained from a cross-combination of irrigation treatment and water source were analyzed. The RW (FI conditions) vs. DW (RDI conditions) OPLS-DA analysis, with one predictive and three orthogonal components (1 + 3 + 0), gave a good model, with a total variance of $R^2X = 0.81$, $R^2Y = 0.978$, and predictability to $Q^2 = 0.951$ (Figure S4a in Supplementary Materials). In the OPLS-DA score plot the olive oil samples were well separated along the predictive component $t[1]$, according to the specific considered combination of irrigation regime and water source. The RW (RDI conditions) vs. DW (FI conditions) OPLS-DA analysis (1 + 3 + 0, $R^2X = 0.716$, $R^2Y = 0.899$ and $Q^2 = 0.707$) showed a clear separation of samples according to the considered irrigation treatment and water source combinations (Figure S4b in Supplementary Materials). The molecular components responsible for separation between olive oil samples were observed by examining the OPLS-DA S-plot (Figure S4a,b in Supplementary Materials). Specifically, in both models, a higher relative content of linoleic (2.74 and 5.34 ppm) and linolenic (2.78 and 5.38 ppm) acids were found in olive oils obtained using the RW water source (FI and RDI regime). Finally, olive oils obtained from DW–RDI were characterized by saturated fatty acids, while a high relative content of oleic acid was found in olive oil obtained by DW–FI.

Since the Q^2 parameter can be considered as a measure of the predictive ability for all the statistical models here obtained, it also gives a synthesis of the differences found between the two classes produced in each model. Thus, a comparison among the obtained Q^2 values for the six different OPLS-DA models is reported in Table S1 in Supplementary Materials. The Q^2 parameters observed for the statistical models obtained comparing all possible irrigation treatment and water source combinations range from a minimal 0.707 to a maximal 0.951 value, obtained for RW–RDI vs. DW–FI and RW–FI vs. DW–RDI, respectively. The corresponding Q^2 parameters of the statistical models obtained discriminating the used water sources (RW, DW) for each defined irrigation strategy showed similar values but with enhanced differences due to water source for FI conditions ($Q^2 = 0.807$ and 0.866 for (RW vs. DW) (RDI conditions) and (RW vs. DW) (FI conditions), respectively). Furthermore, the OPLS-DA models obtained comparing the different irrigation strategies for each used water source showed a similar Q^2 parameter with a more marked difference, due to the irrigation regime in the case of DW use ($Q^2 = 0.817$ and 0.892 for (RDI vs. FI) (RW used source) and (RDI vs. FI) (DW used source) respectively). Interestingly, the highest and lowest Q^2 parameters were observed for OPLS-DA models related to comparison of the cross-exchange irrigation strategy and used water source (RW (FI conditions) vs. DW (RDI conditions) and RW (RDI conditions) vs. DW (FI conditions)). In particular, the model for RW (FI conditions) vs. DW (RDI conditions) showed the highest difference in metabolites discriminating between the two classes with a Q^2 value of 0.951, focusing on the oil major components. On the other hand, a Q^2 parameter of 0.707 indicates the lowest differentiation in the oil major components comparing RW (RDI conditions) vs. DW (FI conditions).

In addition, the quantitative variations in discriminating fatty acids among different irrigation strategies were calculated by the integration of unbiased signals (NMR specific resonances), identified by NMR-based untargeted MVDA and reported in Table S2 in Supplementary Materials. In addition, as an intuitive visualization of the whole data, a Hierarchical Clustering Heatmaps (heatmap) is presented in Figure 2a. Each colored cell on the map corresponds to an average value of fatty acid percentage, in rows, and irrigation strategies in columns.

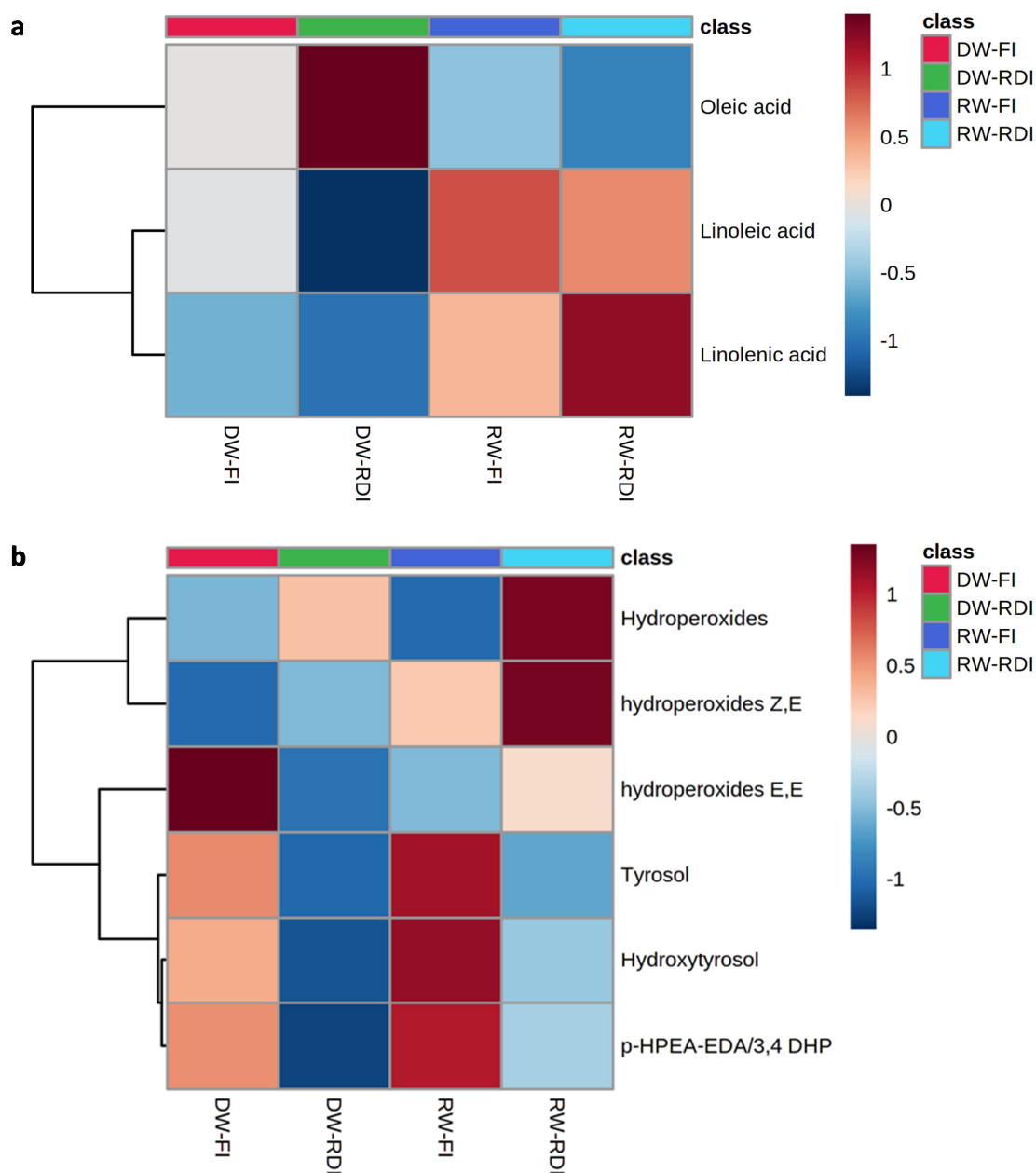


Figure 2. Hierarchical Clustering Heatmaps (heatmap) obtained for the whole data, using Euclidean distance measure and Ward clustering algorithm. Red: “0” time, green: “90” time, blue: “MW” and dark blue: “END” samples, respectively. Color key indicates metabolite values: dark blue: lowest and dark red: highest. (a) Rows: fatty acids and columns: irrigation strategies. (b) Rows: compounds and columns: irrigation strategies.

A pairwise comparison of fatty acids for all conditions was also reported as a Log₂ fold change (FC) ratio and illustrated in Figure 3. In detail, a statistically significant level

of linoleic acid in RW treatment for both irrigation strategies, RDI and FI, with respect to DW treatment was observed. Furthermore, RW–FI and DW–FI showed a statistically significantly higher level of linoleic acid when compared with DW–RDI.

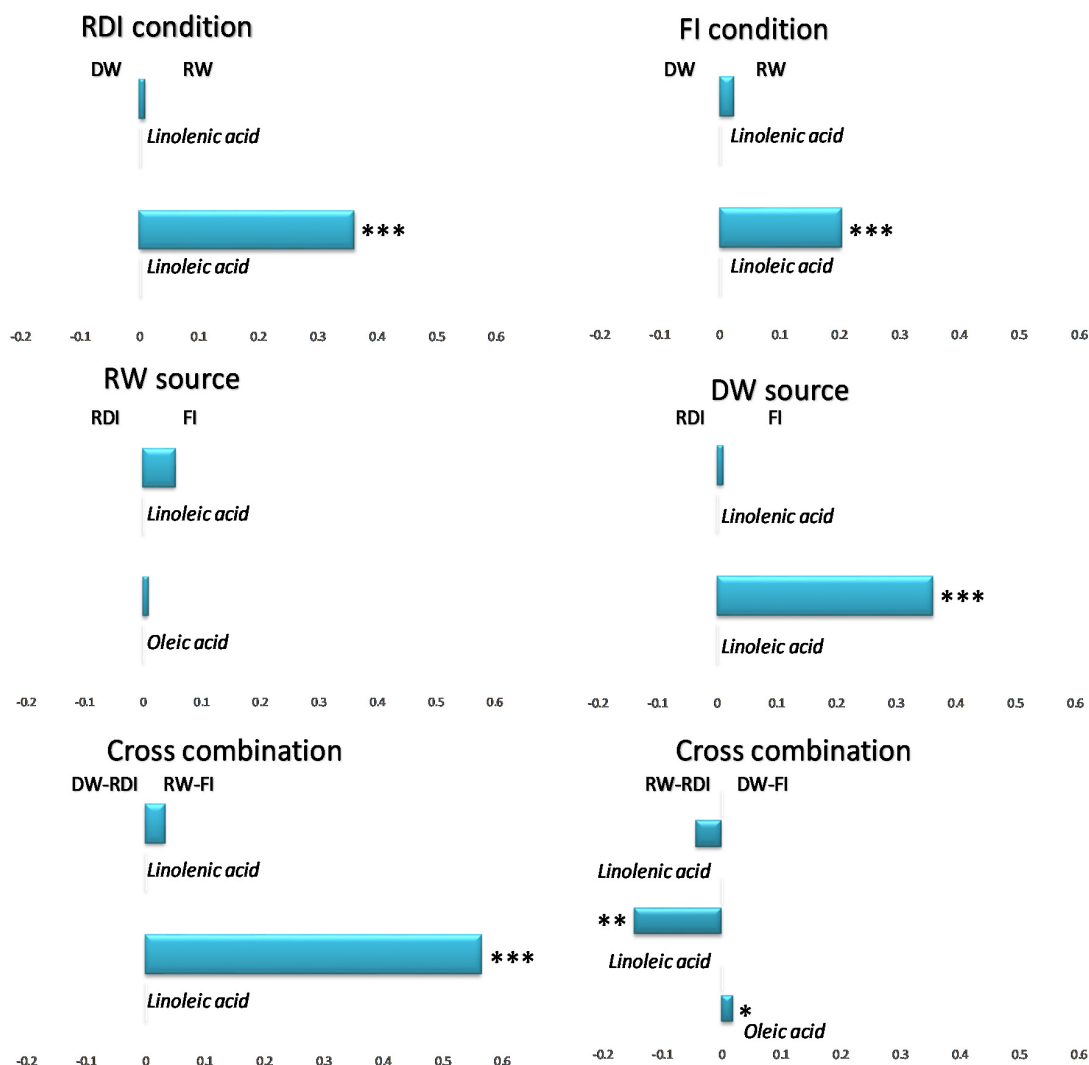


Figure 3. Variation in discriminating fatty acid content for all irrigation strategies (RDI, FI) and water source (RW, DW) combinations. Signif. codes ‘***’ 0.001 ‘**’ 0.01 ‘*’ 0.05.

3.2. MVDA Analysis (PCA and OPLS-DA) on EVOOs Minor Components (BUCKET-2)

The differences between the unaponifiable fraction of olive oil related to the irrigation treatment and water source was then evaluated by the NMR–MVDA of oil minor components (BUCKET-2, bucket table obtained using multisuppressed ^1H NOESYGPPS spectra). Preliminarily, a first level of investigation was performed using the unsupervised analysis. The PCA showed at first glance not only a grouping of samples based on irrigation strategy (FI and RDI), but also a separation according to the used water (RW and DW) (Figure 4a). The observed trend was also confirmed by the supervised analysis (Figure 4b). In the OPLS-DA model (validated by the permutation test, Figure S5 in Supplementary Materials), the corresponding score plot showed that olive oil samples were grouped along the predictive component $t[1]$ clearly according to the irrigation strategy (FI and RDI), while the orthogonal to $t[1]$ component showed a clear separation of samples based on water source used (RW and DW). This suggests, as already observed for the EVOOs major components, the presence of a marked difference, also for the minor components, according not only to the adopted irrigation method but also to used water source. The study of the corresponding

S-plot and S-line of the OPLS-DA score plot (Figure 4c,d) led to the possibility to identify the specific metabolites responsible for the FI and RDI samples separation. In particular, a high relative content of tyrosol, hydroxytyrosol and their derivatives (6.78 and 6.74 ppm, *p*-HPEA-EDA, or oleocanthal and 3,4 DHPEA-EDA or oleacein (9.66 and 9.22 ppm) and hydroperoxides associated with (E,E)-conjugated dienic system (5.78, 5.74 and 5.70 ppm) were found in olive oils obtained from the FI strategy. However, EVOOs obtained from RDI treatment were characterized by higher relative content of hydroperoxides (8.14 and 8.18 ppm) and hydroperoxides associated with a (Z,E)-conjugated dienic system (6.04–5.95 and 6.58–6.54 ppm). The NMR signals responsible for the sample grouping due to oil minor components are also highlighted in the multisuppressed ^1H NOESYGPPS NMR spectrum (Figure S6 in Supplementary Materials).

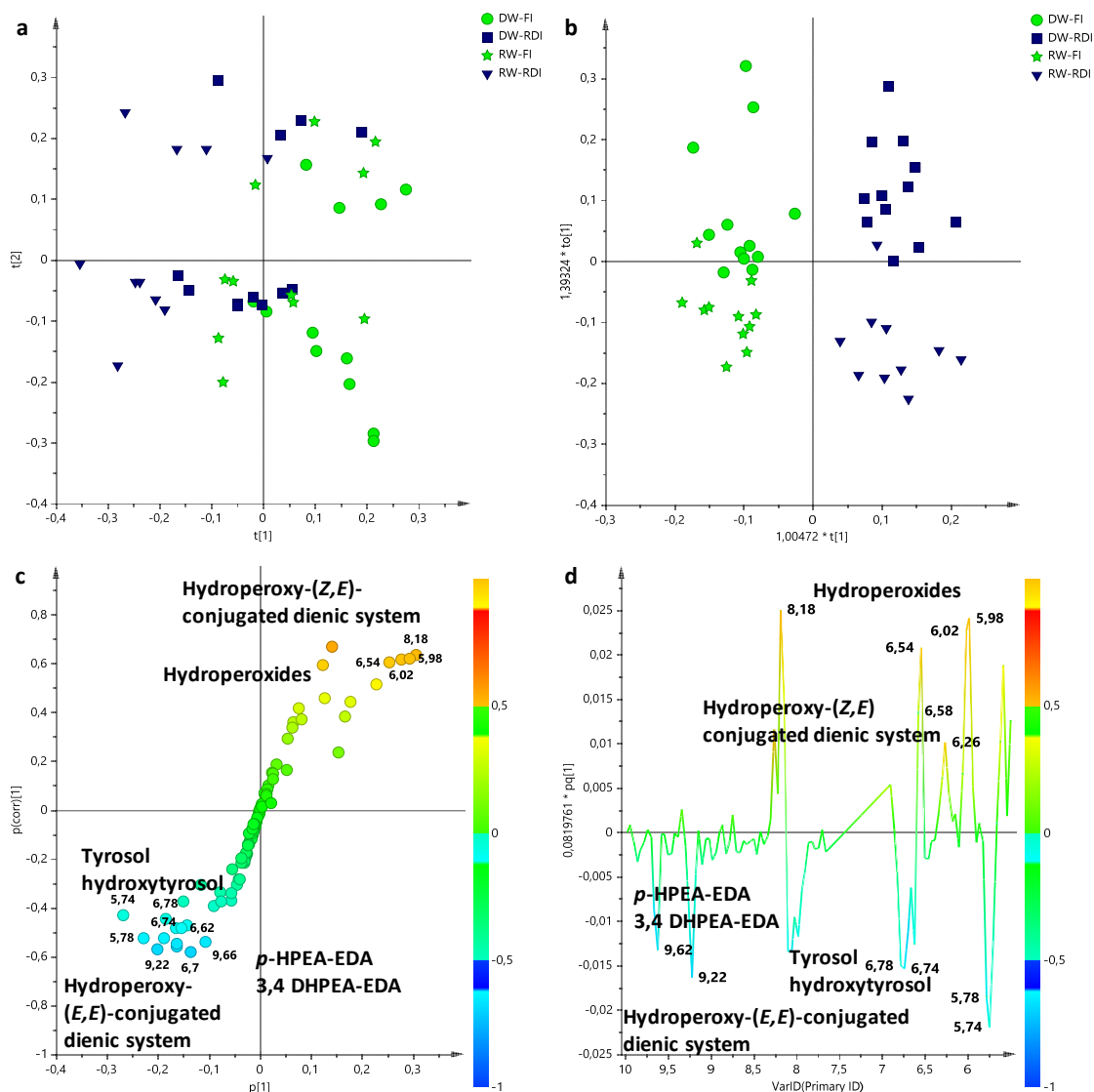


Figure 4. (a) $t[1]/t[2]$ PCA score plot (4 PCs with $R^2X = 0.8$ and $Q^2 = 0.623$) performed on minor components (BUCKET-2) of olive oil samples obtained from two irrigation strategies, FI and RDI. (b) OPLS-DA (1 + 3 + 0 with $R^2X = 0.643$, $R^2Y = 0.893$ and $Q^2 = 0.731$) $t[1]/to[1]$ score plot performed on minor components (BUCKET-2) of olive oil samples obtained from two irrigation strategies, FI and RDI. (c) S-plot for the OPLS-DA model and the variables indicated ppm in the ^1H NMR spectrum. (d) S-line for the OPLS-DA model. Green circle, DW-FI; blue box, DW-RDI; green star, RW-FI and blue triangle, RW-RDI. The variables indicated ppm in the ^1H NMR spectrum.

Pairwise OPLS-DA Analysis According to Irrigation Strategy (RDI, FI) and Water Source (RW, DW) for EVOOs Minor Components (BUCKET-2)

In order to investigate the effect of both irrigation strategies (RDI, FI) and used water source (RW, DW), a supervised pairwise OPLS-DA analysis for all the treatments was applied. As for olive oil major components, six different models were obtained and analyzed.

The (RW vs. DW) (RDI conditions) OPLS-DA analysis (1 + 3 + 0, with $R^2X = 0.741$, $R^2Y = 0.972$ and $Q^2 = 0.844$) showed a good grouping of olive oils samples according to water source, RW and DW, along the predictive component $t[1]$ (Figure S7a in Supplementary Materials). The (RW vs. DW) (FI conditions) OPLS-DA analysis gave a good model with one predictive and three orthogonal components (1 + 3 + 0, $R^2X = 0.688$, $R^2Y = 0.828$ and $Q^2 = 0.564$, Figure S7b in Supplementary Materials), showing, again, the samples grouped according to water source, RW and DW. From analysis of the S-plot, it was possible to identify the metabolites responsible for grouping (Figure S7a,b in Supplementary Materials). In particular, the olive oils obtained using RW as the water source showed a higher relative content of *p*-HPEA-EDA and 3,4 DHPEA-EDA (9.66 and 9.22 ppm) in RDI condition. RW use also showed relatively high levels of hydroperoxy-(Z,E)-conjugated dienic system (6.58–6.54 ppm, 6.04–5.95 ppm) and hydroperoxides (8.18 and 8.14 ppm) compared with olive oils obtained using DW as water source, in both RDI and FI treatments. Furthermore, the oils obtained using DW in FI condition were characterized by a high relative content of hydroperoxides-(E,E)-conjugated dienic system (5.79–5.69 ppm).

Moreover, in order to evaluate the effects of the different irrigation strategies for a single used water source, a supervised analysis was performed obtaining two new models. The (RDI vs. FI) (RW water source) OPLS-DA analysis, (1 + 3 + 0, with $R^2X = 0.801$, $R^2Y = 0.907$ and $Q^2 = 0.625$) displayed a good separation of olive oils according to irrigation strategy, FI and RDI (Figure S7c in Supplementary Materials). The (RDI vs. FI) (DW water source) OPLS-DA score plot analysis (1 + 3 + 0, with $R^2X = 0.705$, $R^2Y = 0.984$ and $Q^2 = 0.831$) also showed a good separation of olive oils according to the applied irrigation strategy (Figure S7d in Supplementary Materials). Analyses of the S-plots (Figure S7c,d in Supplementary Materials) revealed a high relative content of tyrosol, hydroxytyrosol and their derivatives (6.78 and 6.74 ppm), *p*-HPEA-EDA and 3,4 DHPEA-EDA (9.66 and 9.22 ppm) in olive oils obtained from FI treatment using both RW and DW water. On the contrary, higher hydroperoxides (8.18 ppm) and hydroperoxides associated with the (Z,E)-conjugated dienic system (6.04–5.95 ppm, 6.58–6.54 ppm) were discriminating for olive oil obtained under RDI strategy combined with RW and DW. In addition, olive oil obtained from DW-FI showed a higher relative content of hydroperoxides associated with the (E,E)-conjugated dienic system (5.78, 5.74 and 5.70 ppm).

Thereafter, the models obtained with a cross combination of irrigation treatment and water source used were also analyzed. The RW (FI conditions) vs. DW (RDI conditions) OPLS-DA analysis, with one predictive and three orthogonal components (1 + 3 + 0), gave a good model, with a total variance of $R^2X = 0.692$, $R^2Y = 0.968$ and predictability Q^2 of 0.88. In the OPLS-DA score plot, the olive oils obtained from RW (FI conditions) and DW (RDI conditions) were well separated along the predictive component $t[1]$ (Figure S8a in Supplementary Materials). Finally, the RW (RDI conditions) vs. DW (FI conditions) supervised analysis was performed. The OPLS-DA score plot (1 + 3 + 0, $R^2X = 0.731$, $R^2Y = 0.961$ and $Q^2 = 0.74$) showed a good separation between samples of RW (RDI condition) and DW (FI condition) along the predictive component $t[1]$ (Figure S8b in Supplementary Materials). The molecular components responsible for separation between olive oil samples were identified by examining the OPLS-DA S-plot (Figure S8a,b in Supplementary Materials). In particular, higher relative levels of tyrosol, hydroxytyrosol and their derivatives (6.78 and 6.74 ppm) and secoiridoid derivatives, such as *p*-HPEA-EDA and 3,4 DHPEA-EDA (9.66 and 9.22 ppm), were found in olive oils obtained from RW (FI conditions) compared with DW (RDI condition). EVOOs obtained from RW-RDI were characterized by a higher relative content of hydroperoxides (8.14 and 8.18 ppm) and hydroperoxides associated with the (Z,E)-conjugated dienic system (6.04–5.95 ppm, 6.58–6.54 ppm), compared with

olive oils obtained under the DW–FI regime. On the other hand, the higher hydroperoxy-(E,E)-conjugated dienic system (5.78, 5.74 and 5.70 ppm) was characteristics of olive oils obtained from DW (FI conditions).

As already reported for EVOOs major components (BUCKET-1), and minor components (BUCKET-2), the Q^2 parameter can be evaluated as a measure of the predictive ability of the statistical models, also giving a quantitative hint of the difference between the two classes produced by the discriminating metabolites. The obtained Q^2 values of the corresponding OPLS-DA models for all possible irrigation strategies and water source combinations are reported in Table S3 in Supplementary Materials. The Q^2 parameter ranges, in this case, from a minimal 0.564 to a maximal 0.880 value obtained for RW–FI vs. DW–FI and RW–FI vs. DW–RDI, respectively. The Q^2 parameters of OPLS-DA models, obtained discriminating between the used water source (RW, DW) for each irrigation strategy (RDI, FI), showed a marked difference. In particular, the (RW vs. DW) (FI conditions) model was characterized by a low Q^2 parameter (0.564), indicating the lowest differentiation in the olive oil minor components among the considered classes. On the other hand, the (RW vs. DW) (RDI conditions) model showed the highest difference in metabolites discriminating between the two classes, with a Q^2 of 0.844. In this case, the statistical models obtained comparing the irrigation strategies (RDI, FI) for each used water source (RW, DW) also showed a marked difference in Q^2 parameters. In particular, $Q^2 = 0.625$ for the OPLS-DA model comparing (RDI vs. FI) (RW used source) indicates, for these olive oil classes, the lowest differentiation considering the unsaponifiable fraction. A relative high difference in metabolites discriminating between the two classes of olive oil minor components ($Q^2 = 0.831$) was found for the model obtained for (RDI vs. FI) (DW used source). Finally, the OPLS-DA models, obtained for a cross-exchange comparison of irrigation strategy and used water source strategy, also gave different Q^2 values (0.880 and 0.740 for RW (FI conditions) vs. DW (RDI conditions) and RW (RDI conditions) vs. DW (FI conditions), respectively). Furthermore, the variation in discriminating metabolite content for each condition was calculated by the integration of selected distinctive NMR signals. The mean value of the NMR resonance found in the ^1H NOESYGPPS spectra is reported in Table S4 in Supplementary Materials, and the relative Log₂ (FC) is represented in Figure 5. In particular, a statistically significant level of phenolic compounds and hydroperoxydes in RW treatment with respect to DW use was found.

Furthermore, as an intuitive visualization of the whole data, a heatmap is presented in Figure 2b. Each coloured cell on the map corresponds to an average value of selected unbiased NMR signals in rows and irrigation strategies in columns. The absolute values for the molar concentration of secoiridoid derivatives (the sum of p–HPEA–EDA and 3,4 DHPEA–EDA) were also calculated showing a variation in range from 249 mg/kg (in DW–RDI) to 535 mg/kg (in both water sources under FI condition) in accordance with previously reported data for these compounds [40–42].

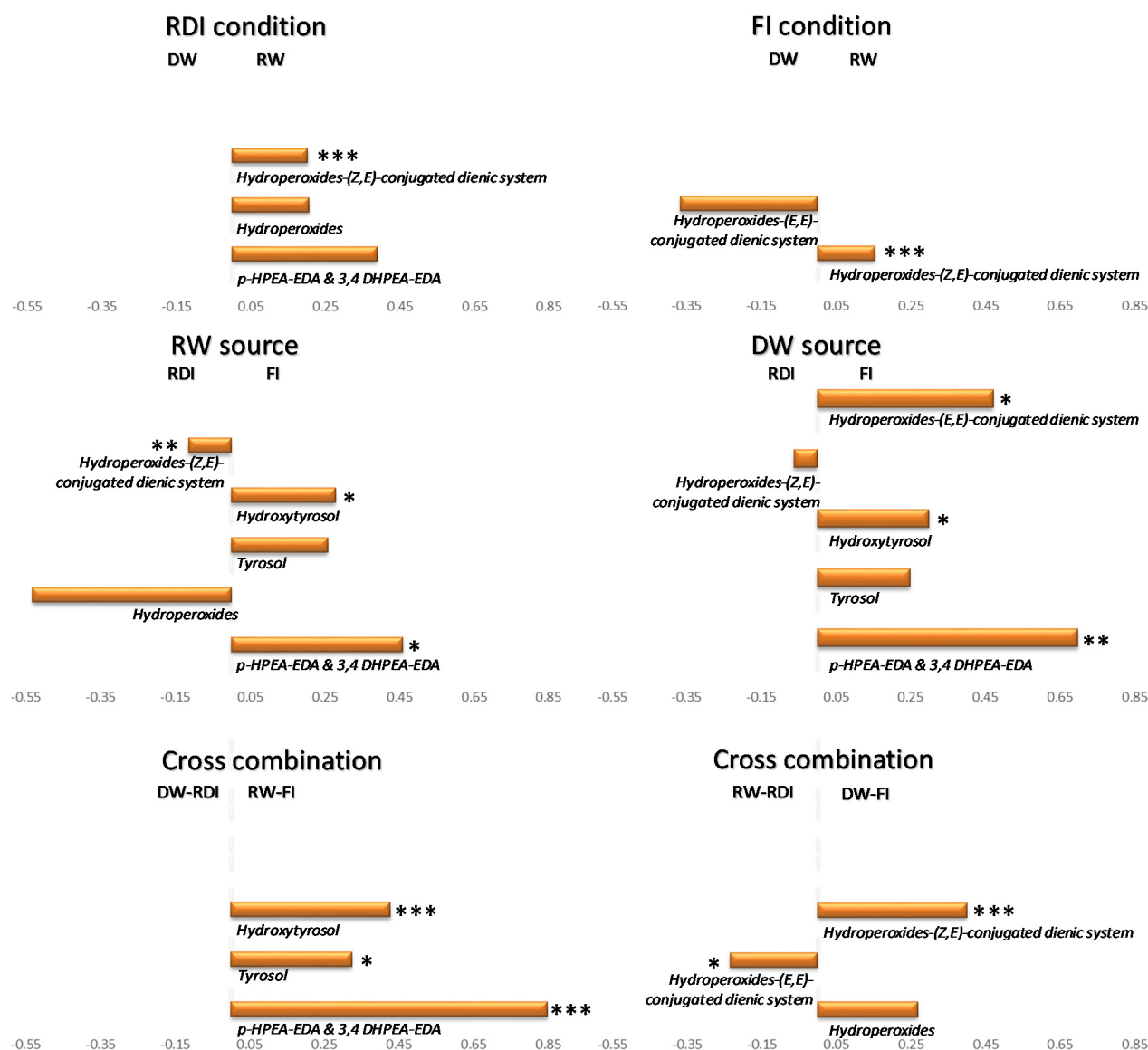


Figure 5. Variation in discriminating metabolites content for all irrigation strategies (RDI, FI) and water source (RW, DW) combinations. Signif. Codes ‘***’ 0.001 ‘**’ 0.01 ‘*’ 0.05.

4. Discussion

This study shows a relevant variability of olive oil profiles evaluated by the ^1H NMR spectroscopy approach in relation to different irrigation strategies, RDI and FI, combined with the use of reclaimed water sources, RW and DW. The results of supervised pairwise analysis OPLS-DA for all the possible treatments are summarized and qualitatively reported in Table S5 in Supplementary Materials. Moreover, only few works studied the metabolic effects of the irrigation with desalinated water (DW) or of the combination of both water sources (DW and RW) with the RDI and FI strategies on cv. Arbosana.

Concerning the olive oil major components, an increase in saturated and a decrease in unsaturated (in particular linoleic) fatty acids under RDI regime was observed. As already reported in the literature, for the cv. Arbequina, the linoleic acid content is mainly related to irrigation strategies [43]. Arbequina trees irrigated with RDI strategy showed a low linoleic acid content with respect to the FI treatment in the mesocarp, demonstrating that the RDI had a negative effect on fatty acid unsaturation [43]. A similar reduction in the linoleic acid content for severely stressed trees was also observed in the same cv. Arbequina when irrigation volumes were 30% less than the control [44]. However, other

authors reported that the fatty acid profiles could be poorly or not influenced by water deficit [44–46]. Therefore, further investigations on the RW–RDI combination are necessary, since insufficient data are reported in the literature [5].

Considering the water quality effect as well, it should be noted that, in both strategies (RDI and FI), the RW with respect to DW use resulted in an increase in unsaturated fatty acids, (linoleic and linolenic acids) as well as an increase in ratio ω_6/ω_3 . According to the literature, data and previous reports by Trigueros 2019, the use of saline water (RW) produced an increase in linoleic acid that could be ascribed to the fatty acid synthase enzymes stimulation during ripening in RW treatment [5,10]. As already observed for cv. Arbosana, a decrease in linoleic acid in olive oil obtained from DW use (DW–RDI and DW–FI) with respect to olive oil obtained from RW (RW–RDI and RW–FI) was found [5], suggesting that the fatty acids composition is mainly influenced by the water quality. In fact, as reported in previous works for different cultivars, the lipid profiles of olive oils were not influenced by the deficit irrigation strategy [7,44].

The oil minor components analysis revealed the presence of phenolic compounds, mainly as tyrosol and hydroxytyrosol and their derivatives, p-HPEA–EDA (or oleocanthal) and 3,4 DHPEA–EDA (or oleacein). The primary oxidation compounds in olive oils were also observed. Generally, these compounds derive from the fatty acid acyl group degradation and can be naturally found in EVOO at low concentration [32]. When compared with DW, the RDI strategy combined with RW showed a relative increase in secoiridoid derivatives and primary oxidation compounds. The presence of these phenolic compounds is in agreement with the literature related to cv. Arbosana, showing an increase in phenolic compounds in RW–RDI treatment [5]. The high phenolic compounds content in RW treatment could also be due to a stress response to the high salt levels [5]. This is consistent with many studies [18,44,46] that demonstrated the water-deficit enhancing synthesis of these compounds in the fruit, according to Alagna et al. (2012) [47]; indeed, severe conditions trigger antioxidation mechanisms activated by the tree in response to oxidative stress, and hence accumulate in oil [48].

Therefore, in RW–RDI, salts and regulated deficit irrigation can be classified as abiotic stress that has a positive effect on some oil minor components. Indeed, phenylalanine ammonia lyase (PAL), an enzyme implicated in polyphenols biosynthesis, is activated by salinity condition. The salt-originated stress, activating the enzyme, causes phenolic compound accumulation in the oil [7,49]. Moreover, as already reported in the literature, water stress also causes a considerable increase in secoiridoid derivatives, inducing PAL activity [42,50–52]. In fact, the synthesis and activity of PAL, not only in olives but also in other fruits, is increased in stressful conditions, including nutrient deficiencies [52]. It was demonstrated that PAL activity and polyphenols content in olive oils decrease with water applied to the olive tree [42,52]. Thus, water deficit increases the PAL activity in olive fruit, enhancing the transfer of phenolic compound from olive paste to olive oil [50].

In addition, RDI combined with RW use showed an increase in hydroperoxides when compared with DW–RDI. This result was already observed in Arbosana olive oils obtained from DW–RDI [5]. However, this aspect needs further investigations, since there are few works hereto comparing the RW–RDI and DW–RDI irrigation treatments. Several studies reported changes in olive oil quality parameters caused by water deficit in different cultivars [5,44,45]. The analysis of minor components of olive oil obtained comparing the two water sources (RW, DW) under FI regime showed the presence of primary oxidation compounds irrespective of the applied water source. In particular, a higher relative content of the hydroperoxy-(Z,E)-conjugated dienic system was observed in RW with respect to DW-related samples. On the contrary, its isomer hydroperoxy-(E,E)-conjugated dienic system was prevalent in DW with respect to RW-related samples. These compounds originate by the oxidative degradation of food lipids. In particular, hydroperoxy groups associated with the (Z,E)-conjugated dienic and hydroperoxy-(E,E)-conjugated dienic systems seem to derive from linoleic groups and oleic acid, respectively [32]. This result is also confirmed by fatty acids quantification, as a higher linoleic acid percentage was in RW–FI with respect

to DW–FI, while higher relative oleic acid percentage was found in DW–FI compared with RW–FI.

Unsaturated fatty acids, mainly oleic acid, as well as phenolic compounds (tyrosol, hydroxytyrosol and their derivatives) are known to be responsible for the beneficial health effects of olive oil [26]. Phenolic compounds, including p–HPEA–EDA and 3,4 DHPEA–EDA, are associated with the beneficial effects of olive oil on human health because of their antioxidant properties together with anticarcinogenic, anti-inflammatory, antimicrobial, antihypertensive, antidyslipidemic, cardioprotective, laxative, and antiplatelet effects [50]. Furthermore, p–HPEA–EDA, 3,4 DHPEA–EDA, tyrosol and hydroxytyrosol are responsible for organoleptic characteristics and are related to the shelf life of olive oils [50]. Several works demonstrated that olive oil bitterness, astringency and pungency were due to phenolic composition [20]. For example, the “pungent” and “bitter” characteristics were attributed to the presence of tyrosol, hydroxytyrosol and their derivatives [20,50]. Moreover, oxidative stability seems to be related to 3,4 DHPEA–EDA content [50]. Tyrosol and hydroxytyrosol are largely known for their antioxidant activity [26]. In particular, hydroxytyrosol is involved in several biological effects, such as cardio-protective, anticancer, neuroprotective antimicrobial and others [26]. The secoiridoid compounds were produced during oil extraction by hydrolysis, catalyzed by the β -glucosidases of oleuropein and ligustrosin [20]. Other minor components, such as carotenoids, phytosterols and tocopherols showing slight differences in the pairwise evaluation of the present study, contribute to olive oil’s nutritional value. Carotenoids contribute to olive oil stability because of their antioxidant properties. Pigments are also responsible for olive oil color, one of the major characteristics for the consumer’s perception of quality. Moreover, chlorophylls and carotenoids play an important role in oxidative stability due to their antioxidant nature in the dark and pro-oxidant activity in the light.

In conclusion, in this study for the first time, the effects of two different irrigation strategies, two different water qualities and their combination on the metabolic profiles of monovarietal EVOOs were analysed by ^1H NMR combined with MVDA. The fatty acid composition was mainly influenced by the water quality. In particular, EVOOs obtained from RW use showed an increase in unsaturated fatty acids, ω_6/ω_3 ratio and polyphenols content when compared with DW water. On the other hand, an increase in saturated and a decrease in unsaturated (oleic, linoleic and linolenic) fatty acids under RDI regime was observed. Moreover, RDI combined with RW use showed an increase in hydroperoxides and secoiridoid derivatives when compared with DW–RDI. Thus, the right combination of two abiotic stressors, such as deficit irrigation strategy and reclaimed water source, is important in order to guarantee the olive oil shelf life and nutraceutical properties of EVOOs. Further investigations on other cultivars are needed to better characterize the effect of the use of unconventional water sources combined with different irrigation techniques. Nevertheless, these preliminary results could be important in providing a useful tool for managing the problem of water scarcity and guaranteeing the high health values of olive oil. An irrigation technique, based on deficit irrigation and saline reclaimed irrigation water use, could optimize crop management in olive trees where environmental sustainability represents a key factor.

Supplementary Materials: The following supporting information can be downloaded at: <https://www.mdpi.com/article/10.3390/su14031592/s1>, Figure S1. Permutation test performed with 20 cycles of random permutation of Y variables on OPLS-DA analysis for each model obtained for major components of EVOOs (BUCKET-1). The horizontal axis shows the correlation between the original and permuted y. The vertical axis shows the values for R2 (green line) and Q2 (blue line). The intercept is a measure of the overfit. Steep slope indicates good fit. Figure S2. Comparison of S-line plot obtained for major component (BUCKET-1) and ^1H ZG NMR spectrum of olive oil in CDCl₃ obtained at 400 MHz. The main resonances (NMR signals) responsible for the olive oil separation were marked in the spectrum. Figure S3. Pairwise OPLS-DA analysis obtained for major components (BUCKET-1) of EVOOs. (a) OPLS-DA t[1]/to[1] score plot of EVOOs obtained from (RW vs. DW) in RDI conditions and relative S-plot. (b) OPLS-DA t[1]/to[1] score plot of EVOOs obtained from

(RW vs. DW) in FI conditions and relative S-plot. (c) OPLS-DA $t[1]/to[1]$ score plot of EVOOs obtained from (RDI vs. FI) (RW used source) and relative S-plot. (d) OPLS-DA $t[1]/to[1]$ score plot EVOOs obtained from (RDI vs. FI) (DW used source) and relative S-plot for the model. Blue box, DW–RDI; blue triangle, RW–RDI; green circle DW–FI; green star, RW–FI. The variables indicated ppm in the ^1H NMR spectrum. Figure S4. Pairwise OPLS-DA analysis obtained for major components (BUCKET-1) of EVOOs. (a) OPLS-DA $t[1]/to[1]$ score plot of EVOOs obtained from RW (FI conditions) vs. DW (RDI conditions) and relative S-plot. Green star, RW–FI; blue box, DW–RDI. (b) OPLS-DA $t[1]/to[1]$ score plot of EVOOs obtained from RW (RDI conditions) vs. DW (FI conditions) and relative S-plot. Green circle, DW–FI; blue triangle, RW–RDI. The variables indicated ppm in the ^1H NMR spectrum. Figure S5. Permutation test performed with 20 cycles of random permutation of Y variables on OPLS-DA analysis for each model, obtained for minor component of EVOOs (BUCKET-2). The horizontal axis shows the correlation between the original and permuted y. The vertical axis shows the values for R^2 (green line) and Q^2 (blue line). The intercept is a measure of the overfit. Steep slope indicates good fit. Figure S6. Comparison of S-line plot obtained for minor component (BUCKET-2) and expansion of 1D NOESYGPPS NMR spectrum of olive oil in CDCl₃ obtained at 400MHz. The signals responsible for the sample separation were indicated in the spectrum. Figure S7. Pairwise OPLS-DA analysis obtained for minor components (BUCKET-2) of EVOOs. (a) OPLS-DA $t[1]/to[1]$ score plot of EVOOs obtained from (RW vs. DW) in RDI conditions and relative S-plot. (b) OPLS-DA $t[1]/to[1]$ score plot of EVOOs obtained from (RW vs. DW) in FI conditions and relative S-plot. (c) OPLS-DA $t[1]/to[1]$ score plot of EVOOs obtained from (RDI vs. FI) (RW used source) and relative S-plot. (d) OPLS-DA $t[1]/to[1]$ score plot EVOOs obtained from (RDI vs. FI) (DW used source) and relative S-plot. Blue box, DW–RDI; blue triangle, RW–RDI; green circle DW–FI; green star, RW–FI. The variables indicated ppm in the ^1H NMR spectrum. Figure S8. Pairwise OPLS-DA analysis obtained for minor components (BUCKET-2) of EVOOs. (a) OPLS-DA $t[1]/to[1]$ score plot of EVOOs obtained from RW (FI conditions) vs. DW (RDI conditions) and relative S-plot. Green star, RW–FI; blue box, DW–RDI. (b) OPLS-DA $t[1]/to[1]$ score plot of EVOOs obtained from RW (RDI conditions) vs. DW (FI conditions) and relative S-plot. Green circle, DW–FI; blue triangle, RW–RDI. The variables indicated ppm in the ^1H NMR spectrum. Table S1. Predictability (Q^2) values for supervised pairwise analysis OPLS-DA for all the possible treatments combination. (RW vs. DW) (RDI conditions); (RW vs. DW) (FI conditions); (RDI vs. FI) (RW used source); (RDI vs. FI) (DW used source); RW (FI conditions) vs. DW (RDI conditions) and RW (RDI conditions) vs. DW (FI conditions). Table S2. Fatty acid percentage calculated by integration of unbiased signals in the ^1H ZG NMR spectra. Different letters within the same row indicate significant differences among treatments for the fatty acids according to ANOVA with Tukey's honestly significant differences (HSD) post hoc test; p value < 0.05. Table S3. Predictability (Q^2) values for supervised pairwise analysis OPLS-DA for all the possible treatments combination. (RW vs. DW) (RDI conditions); (RW vs. DW) (FI conditions); (RDI vs. FI) (RW used source); (RDI vs. FI) (DW used source); RW (FI conditions) vs. DW (RDI conditions) and RW (RDI conditions) vs. DW (FI conditions). Table S4. Mean \pm SD of selected unbiased signals in ^1H NOESYGPPS NMR spectra. Different letters within the same row indicate significant differences among treatments for the polyphenols according to ANOVA with Tukey's honestly significant differences (HSD) post hoc test; p value < 0.05. Table S5. Results of supervised pairwise analysis OPLS-DA for all the possible treatments. (RW vs. DW) (RDI conditions); (RW vs. DW) (FI conditions); (RDI vs. FI) (RW water source); (RDI vs. FI) (DW water source); RW (FI conditions) vs. DW (RDI conditions); RW (RDI conditions) vs. DW (FI conditions). “ \uparrow ” major relative content; “ \downarrow ” minor relative content.

Author Contributions: F.A.: investigation, formal analysis, writing—original draft, writing—review and editing; C.R.G.: investigation, software and data curation; L.D.C.: investigation, software and data curation; G.C.: investigation and data curation; G.L.: investigation and data curation; S.C.: funding acquisition, conceptualization and methodology; G.A.V.: funding acquisition, conceptualization and methodology supervision; F.P.F.: methodology, writing—review, editing and supervision. All authors have read and agreed to the published version of the manuscript.

Funding: This research was co-funded by the Regione Puglia as the project “Sistema innovativo di monitoraggio e trattamento delle acque reflue per il miglioramento della compatibilità ambientale ai fini di un’agricoltura sostenibile”-SMART WATER (No. 5ABY6P0) through the INNONETWORK CALL 2017. The research involved in this work has been supported by the EU and Water JPI for funding, in the frame of the collaborative international Consortium DESERT, financed under the

ERA-NET WaterWorks 2014 Cofunded Call. This ERA-NET is an integral part of the 2015 Joint Activities developed by the Water Challenges for a Changing World Joint Programme Initiative (Water JPI).

Institutional Review Board Statement: Not applicable.

Informed Consent Statement: Not applicable.

Data Availability Statement: Data is contained within the article and in the supplementary material.

Acknowledgments: C.R.G. (AIM-1882733-1) thanks Programma Operativo Nazionale (PON) Ricerca e Innovazione 2014–2020 Asse I “Capitale Umano”, Azione I.2, Avviso “A.I.M: Attraction and International Mobility”.

Conflicts of Interest: The authors declare no conflict of interest.

References

- World Economic Forum. *The Global Risks Report 2020*, 15th ed.; World Economic Forum: Cologny, Switzerland, 2020.
- Vivaldi, G.A.; Camposeo, S.; Lopriore, G.; Romero-Trigueros, C.; Salcedo, F.P. Using saline reclaimed water on almond grown in mediterranean conditions: Deficit irrigation strategies and salinity effects. *Water Supply* **2019**, *19*, 1413–1421. [[CrossRef](#)]
- Arborea, S.; Giannoccaro, G.; De Gennaro, B.C.; Iacobellis, V.; Piccinni, A.F. Cost-benefit analysis of wastewater reuse in Puglia, Southern Italy. *Water* **2017**, *9*, 175. [[CrossRef](#)]
- Pedrero, F.; Camposeo, S.; Pace, B.; Cefola, M.; Vivaldi, G.A. Use of reclaimed wastewater on fruit quality of Nectarine in Southern Italy. *Agric. Water Manag.* **2018**, *203*, 186–192. [[CrossRef](#)]
- Romero-Trigueros, C.; Vivaldi, G.A.; Nicolás, E.N.; Paduano, A.; Salcedo, F.P.; Camposeo, S. Ripening indices, olive yield and oil quality in response to irrigation with saline reclaimed water and deficit strategies. *Front. Plant Sci.* **2019**, *10*, 1243. [[CrossRef](#)]
- Romero-Trigueros, C.; Parra, M.; Bayona, J.M.; Nortes, P.A.; Alarcón, J.J.; Nicolás, E. Effect of deficit irrigation and reclaimed water on yield and quality of grapefruits at harvest and postharvest. *LWT-Food Sci. Technol.* **2017**, *85*, 405–411. [[CrossRef](#)]
- Romero-Trigueros, C.; Bayona Gambín, J.M.; Nortes Tortosa, P.A.; Alarcón Cabañero, J.J.; Nicolás Nicolás, E. Determination of crop water stress index by infrared thermometry in grapefruit trees irrigated with saline reclaimed water combined with deficit irrigation. *Remote Sens.* **2019**, *11*, 757. [[CrossRef](#)]
- Nicolás, E.; Alarcón, J.; Mounzer, O.; Pedrero, F.; Nortes, P.; Alcobendas, R.; Romero-Trigueros, C.; Bayona, J.; Maestre-Valero, J. Long-term physiological and agronomic responses of mandarin trees to irrigation with saline reclaimed water. *Agric. Water Manag.* **2016**, *166*, 1–8. [[CrossRef](#)]
- Romero Trigueros, C.; Nortes Tortosa, P.A.; Alarcón Cabañero, J.J.; Nicolás Nicolás, E. Determination of ¹⁵N stable isotope natural abundances for assessing the use of saline reclaimed water in grapefruit. *Environ. Eng. Manag. J.* **2014**, *13*, 2525–2530. [[CrossRef](#)]
- Bedbabis, S.; Ferrara, G. Effects of long term irrigation with treated wastewater on leaf mineral element contents and oil quality in olive cv. chemlali. *J. Hortic. Sci. Biotechnol.* **2018**, *93*, 216–223. [[CrossRef](#)]
- Kchaou, H.; Larbi, A.; Gargouri, K.; Chaieb, M.; Morales, F.; Msallem, M. Assessment of tolerance to NaCl salinity of five olive cultivars, based on growth characteristics and Na⁺ and Cl⁻ exclusion mechanisms. *Sci. Hortic.* **2010**, *124*, 306–315. [[CrossRef](#)]
- Ayoub, S.; Al-Shdiefat, S.; Rawashdeh, H.; Bashabsheh, I. Utilization of reclaimed wastewater for olive irrigation: Effect on soil properties, tree growth, yield and oil content. *Agric. Water Manag.* **2016**, *176*, 163–169. [[CrossRef](#)]
- Ben-Gal, A.; Beiersdorf, I.; Yermiyahu, U.; Soda, N.; Presnov, E.; Zipori, I.; Ramirez Crisostomo, R.; Dag, A. Response of young bearing olive trees to irrigation-induced salinity. *Irrig. Sci.* **2017**, *35*, 99–109. [[CrossRef](#)]
- Erel, R.; Eppel, A.; Yermiyahu, U.; Ben-Gal, A.; Levy, G.; Zipori, I.; Schaumann, G.E.; Mayer, O.; Dag, A. Long-term irrigation with reclaimed wastewater: Implications on nutrient management, soil chemistry and olive (*Olea Europaea* L.) performance. *Agric. Water Manag.* **2019**, *213*, 324–335. [[CrossRef](#)]
- Clodoveo, M.L.; Camposeo, S.; De Gennaro, B.; Pascuzzi, S.; Roselli, L. In the ancient world, virgin olive oil was called “liquid gold” by Homer and “the great healer” by Hippocrates. Why has this mythic image been forgotten? *Food Res. Int.* **2014**, *62*, 1062–1068. [[CrossRef](#)]
- Boskou, D.; Camposeo, S.; Clodoveo, M.L. Table olives as sources of bioactive compounds. In *Olive and Olive Oil Bioactive Constituents*; Boskou, D., Ed.; AOCS Press: Urbana, IL, USA, 2015; pp. 217–259, ISBN 978-1-63067-041-2.
- Hernández, M.L.; Velázquez-Palmero, D.; Sicardo, M.D.; Fernández, J.E.; Diaz-Espejo, A.; Martínez-Rivas, J.M. Effect of a regulated deficit irrigation strategy in a hedgerow ‘arbequina’ olive orchard on the mesocarp fatty acid composition and desaturase gene expression with respect to olive oil quality. *Agric. Water Manag.* **2018**, *204*, 100–106. [[CrossRef](#)]
- Rosecrance, R.C.; Krueger, W.H.; Milliron, L.; Bloese, J.; Garcia, C.; Mori, B. Moderate regulated deficit irrigation can increase olive oil yields and decrease tree growth in super high density ‘arbequina’ olive orchards. *Sci. Hortic.* **2015**, *190*, 75–82. [[CrossRef](#)]
- Gucci, R.; Caruso, G.; Gennai, C.; Esposto, S.; Urbani, S.; Servili, M. Fruit growth, yield and oil quality changes induced by deficit irrigation at different stages of olive fruit development. *Agric. Water Manag.* **2019**, *212*, 88–98. [[CrossRef](#)]

20. Servili, M.; Esposto, S.; Fabiani, R.; Urbani, S.; Taticchi, A.; Mariucci, F.; Selvaggini, R.; Montedoro, G.F. Phenolic compounds in olive oil: Antioxidant, health and organoleptic activities according to their chemical structure. *Inflammopharmacol* **2009**, *17*, 76–84. [[CrossRef](#)]
21. Clodoveo, M.L.; Camposeo, S.; Amirante, R.; Dugo, G.; Cicero, N.; Boskou, D. Research and innovative approaches to obtain virgin olive oils with a higher level of bioactive constituents. In *Olive and Olive Oil Bioactive Constituents*; Boskou, D., Ed.; AOCS Press: Urbana, IL, USA, 2015; pp. 179–215, ISBN 978-1-63067-041-2.
22. Bedbabis, S.; Trigui, D.; Ben Ahmed, C.; Clodoveo, M.L.; Camposeo, S.; Vivaldi, G.A.; Ben Rouina, B. Long-terms effects of irrigation with treated municipal wastewater on soil, yield and olive oil quality. *Agric. Water Manag.* **2015**, *160*, 14–21. [[CrossRef](#)]
23. Dag, A.; Kerem, Z.; Yogev, N.; Zipori, I.; Lavee, S.; Ben-David, E. Influence of time of harvest and maturity index on olive oil yield and quality. *Sci. Hortic.* **2011**, *127*, 358–366. [[CrossRef](#)]
24. Matos, L.C.; Cunha, S.C.; Amaral, J.S.; Pereira, J.A.; Andrade, P.B.; Seabra, R.M.; Oliveira, B.P.P. Chemometric characterization of three varietal olive oils (Cvs. Cobrançosa, Madural and Verdeal Transmontana) extracted from olives with different maturation indices. *Food Chem.* **2007**, *102*, 406–414. [[CrossRef](#)]
25. Camposeo, S.; Vivaldi, G.A.; Gattullo, C.E. Ripening indices and harvesting times of different olive cultivars for continuous harvest. *Sci. Hortic.* **2013**, *151*, 1–10. [[CrossRef](#)]
26. Karković Marković, A.; Torić, J.; Barbarić, M.; Jakobušić Brala, C. Hydroxytyrosol, tyrosol and derivatives and their potential effects on human health. *Molecules* **2019**, *24*, 2001. [[CrossRef](#)] [[PubMed](#)]
27. Martín-Peláez, S.; Covas, M.I.; Fitó, M.; Kušar, A.; Pravst, I. Health effects of olive oil polyphenols: Recent advances and possibilities for the use of health claims. *Mol. Nutr. Food Res.* **2013**, *57*, 760–771. [[CrossRef](#)] [[PubMed](#)]
28. Cicerale, S.; Conlan, X.A.; Sinclair, A.J.; Keast, R.S.J. Chemistry and health of olive oil phenolics. *Crit. Rev. Food Sci. Nutr.* **2008**, *49*, 218–236. [[CrossRef](#)] [[PubMed](#)]
29. Abreu, A.C.; Aguilera-Sáez, L.M.; Peña, A.; García-Valverde, M.; Marín, P.; Valera, D.L.; Fernández, I. NMR-based metabolomics approach to study the influence of different conditions of water irrigation and greenhouse ventilation on zucchini crops. *J. Agric. Food Chem.* **2018**, *66*, 8422–8432. [[CrossRef](#)]
30. Girelli, C.R.; Coco, L.D.; Fanizzi, F.P. ¹H NMR spectroscopy and multivariate analysis as possible tool to assess cultivars, from specific geographical areas, in EVOOs. *Eur. J. Lipid Sci. Technol.* **2016**, *118*, 1380–1388. [[CrossRef](#)]
31. Del Coco, L.; Girelli, C.R.; Angilè, F.; Mascio, I.; Montemurro, C.; Distaso, E.; Tamburrano, P.; Chiurlia, S.; Clodoveo, M.L.; Corbo, F.; et al. NMR-based metabolomic study of apulian coratina extra virgin olive oil extracted with a combined ultrasound and thermal conditioning process in an industrial setting. *Food Chem.* **2021**, *345*, 128778. [[CrossRef](#)]
32. Martínez-Yusta, A.; Goicoechea, E.; Guillén, M.D. A review of thermo-oxidative degradation of food lipids studied by ¹H NMR spectroscopy: Influence of degradative conditions and food lipid nature. *Compr. Rev. Food Sci. Food Saf.* **2014**, *13*, 838–859. [[CrossRef](#)]
33. Ruiz-Aracama, A.; Goicoechea, E.; Guillén, M.D. Direct study of minor extra-virgin olive oil components without any sample modification. ¹H NMR multisuppression experiment: A powerful tool. *Food Chem.* **2017**, *228*, 301–314. [[CrossRef](#)]
34. Barison, A.; Grandizoli, C.; Campos, F.; Simonelli, F.; Lenz, C.; Ferreira, A. A simple methodology for the determination of fatty acid composition in edible oils through ¹H NMR spectroscopy. *Magn. Reson. Chem.* **2010**, *48*, 642–650. [[CrossRef](#)]
35. R Development Core Team. *R: A Language and Environment for Statistical Computing*; R Foundation for Statistical Computing: Vienna, Austria, 2013. Available online: <https://www.gbif.org/tool/81287/r-a-language-and-environment-for-statistical-computing-cercacongoogle> (accessed on 30 November 2020).
36. Hammerl, R.; Frank, O.; Hofmann, T. Differential off-line LC-NMR (DOLC-NMR) metabolomics to monitor tyrosine-induced metabolome alterations in *Saccharomyces Cerevisiae*. *J. Agric. Food Chem.* **2017**, *65*, 3230–3241. [[CrossRef](#)] [[PubMed](#)]
37. Angilè, F.; Del Coco, L.; Girelli, C.R.; Basso, L.; Rizzo, L.; Piraino, S.; Stabili, L.; Fanizzi, F.P. ¹H NMR metabolic profile of scyphomedusa *Rhizostoma pulmo* (Scyphozoa, Cnidaria) in Female gonads and somatic tissues: Preliminary results. *Molecules* **2020**, *25*, 806. [[CrossRef](#)] [[PubMed](#)]
38. Girelli, C.R.; Calò, F.; Angilè, F.; Mazzi, L.; Barbini, D.; Fanizzi, F.P. ¹H NMR spectroscopy to characterize Italian extra virgin olive oil blends, using statistical models and databases based on monocultivar reference oils. *Foods* **2020**, *9*, 1797. [[CrossRef](#)] [[PubMed](#)]
39. Alonso-Salces, R.M.; Moreno-Rojas, J.M.; Holland, M.V.; Reniero, F.; Guillou, C.; Héberger, K. Virgin olive oil authentication by multivariate analyses of ¹H NMR fingerprints and $\delta^{13}\text{C}$ and $\delta^2\text{H}$ data. *J. Agric. Food Chem.* **2010**, *58*, 5586–5596. [[CrossRef](#)] [[PubMed](#)]
40. Gomez-Casati, D.F.; Zanol, M.I.; Busi, M.V. Metabolomics in Plants and Humans: Applications in the Prevention and Diagnosis of Diseases. Available online: <https://www.hindawi.com/journals/bmri/2013/792527/> (accessed on 6 November 2019).
41. Gómez-Rico, A.; Salvador, M.D.; La Greca, M.; Fregapane, G. Phenolic and volatile compounds of extra virgin olive oil (*Olea Europaea* L. cv. Cornicabra) with regard to fruit ripening and irrigation management. *J. Agric. Food Chem.* **2006**, *54*, 7130–7136. [[CrossRef](#)] [[PubMed](#)]
42. Servili, M.; Esposto, S.; Lodolini, E.; Selvaggini, R.; Taticchi, A.; Urbani, S.; Montedoro, G.; Serravalle, M.; Gucci, R. Irrigation effects on quality, phenolic composition, and selected volatiles of virgin olive oils cv. leccino. *J. Agric. Food Chem.* **2007**, *55*, 6609–6618. [[CrossRef](#)] [[PubMed](#)]

43. Hernandez-Santana, V.; Fernandes, R.D.M.; Perez-Arcoiza, A.; Fernández, J.E.; Garcia, J.M.; Diaz-Espejo, A. Relationships between fruit growth and oil accumulation with simulated seasonal dynamics of leaf gas exchange in the olive tree. *Agric. For. Meteorol.* **2018**, *256–257*, 458–469. [[CrossRef](#)]
44. Gómez Del Campo, M.; García, J.M. Summer deficit-irrigation strategies in a hedgerow olive cv. arbequina orchard: Effect on oil quality. *J. Agric. Food Chem.* **2013**, *61*, 8899–8905. [[CrossRef](#)] [[PubMed](#)]
45. Caruso, G.; Gucci, R.; Urbani, S.; Esposto, S.; Taticchi, A.; Di Maio, I.; Selvaggini, R.; Servili, M. Effect of different irrigation volumes during fruit development on quality of virgin olive oil of cv. frantoio. *Agric. Water Manag.* **2014**, *134*, 94–103. [[CrossRef](#)]
46. Caruso, G.; Gucci, R.; Sifola, M.I.; Selvaggini, R.; Urbani, S.; Esposto, S.; Taticchi, A.; Servili, M. Irrigation and fruit canopy position modify oil quality of olive trees (cv. Frantoio). *J. Sci. Food Agric.* **2017**, *97*, 3530–3539. [[CrossRef](#)] [[PubMed](#)]
47. Alagna, F.; Mariotti, R.; Panara, F.; Caporali, S.; Urbani, S.; Veneziani, G.; Esposto, S.; Taticchi, A.; Rosati, A.; Rao, R.; et al. Olive phenolic compounds: Metabolic and transcriptional profiling during fruit development. *BMC Plant Biol.* **2012**, *12*, 162. [[CrossRef](#)] [[PubMed](#)]
48. Tietel, Z.; Dag, A.; Yermiyahu, U.; Zipori, I.; Beiersdorf, I.; Krispin, S.; Ben-Gal, A. Irrigation-induced salinity affects olive oil quality and health-promoting properties. *J. Sci. Food Agric.* **2019**, *99*, 1180–1189. [[CrossRef](#)] [[PubMed](#)]
49. Patumi, M.; d’Andria, R.; Marsilio, V.; Fontanazza, G.; Morelli, G.; Lanza, B. Olive and olive oil quality after intensive monocone olive growing (*Olea Europaea* L., cv. Kalamata) in different irrigation regimes. *Food Chem.* **2002**, *77*, 27–34. [[CrossRef](#)]
50. Sena-Moreno, E.; Cabrera-Bañegil, M.; Pérez-Rodríguez, J.M.; Miguel, C.D.; Prieto, M.H.; Martín-Vertedor, D. Influence of water deficit in bioactive compounds of olive paste and oil content. *J. Am. Oil Chem. Soc.* **2018**, *95*, 349–359. [[CrossRef](#)]
51. Martinelli, F.; Basile, B.; Morelli, G.; d’Andria, R.; Tonutti, P. Effects of irrigation on fruit ripening behavior and metabolic changes in olive. *Sci. Hortic.* **2012**, *144*, 201–207. [[CrossRef](#)]
52. Tovar, M.J.; Romero, M.P.; Girona, J.; Motilva, M.J. L-phenylalanine ammonia-lyase activity and concentration of phenolics in developing olive (*Olea Europaea* L cv Arbequina) fruit grown under different irrigation regimes. *J. Sci. Food Agric.* **2002**, *82*, 892–898. [[CrossRef](#)]